Improving End-to-End Pecan Cracking and Shelling by Quantifying Cracks Produced using Different Impactor Geometries

By

Mark William Jackson

(Under the Direction of R. Benjamin Davis)

Abstract

During the industrial pecan cracking and shelling process, kernels are often damaged. To address this problem, a study is conducted to experimentally determine the effect of impactor geometry for end-to-end pecan cracking. In parallel, a software program is developed quantitatively assess the performance of each impactor. Four impactors of varying internal angles (from 30° to 52.5°, in increments of 7.5°) are tested. After cracking, the pecans are passed through a software program that detects, classifies, and measures the pecan cracks using image processing techniques. The software is calibrated and validated using sets of 30 and 380 pecans, respectively. With the validation set, the software accurately detected 90.6% of cracks, classified cracks with an accuracy of 98.7%, and produced crack measurements within 10% of manual measurements. Using this software, pecan impactors are analyzed by categorizing each pecan into one of four categories: under crack, standard crack, ideal crack, or over crack. Cracked and ideally cracked pecans are preferred for their processability, so impactor geometries are then evaluated on the basis of their ability to maximize these crack types across the widest impact energy range. For the four impactors tested, the 30° impactor is found to produce preferred cracks more consistently in a larger energy range relative to the other impactors.

Index Words: Tree nut processing, pecan cracking, kernel damage, pecan shelling, crack detection, image processing, crack quantification, machine vision

Improving End-to-End Pecan Cracking and Shelling by Quantifying Cracks Produced using Different Impactor Geometries

By

Mark William Jackson

B.S., The University of Georgia, 2022

A Thesis Submitted to the Graduate Faculty of The University of Georgia
in Partial Fulfillment of the Requirements for the Degree

Master of Science

Athens, Georgia

2024

Improving End-to-End Pecan Cracking and Shelling by Quantifying Cracks Produced using Different Impactor Geometries

By

Mark William Jackson

Major Professor: R. Benjamin Davis

Committee: Xianqiao (XQ) Wang
Eliza A. Banu

Electronic Version Approved:

Ron Walcott
Vice Provost for Graduate Education and Dean of the Graduate School
The University of Georgia
December 2024

Acknowledgments

Navigating this project proved to be more difficult than anticipated and required some creativity to arrive at the results presented in this thesis. I found myself taking an unexpected career turn, tasked with improving the cracking and shelling processes of pecans, but as my advisor told me entering this project, “Things tend to get more interesting the further invested you get.” This project was no exception, and with the guidance of Dr. Davis, I can say that I am proud of what I have accomplished for this project. I would like to thank Dr. Davis for his involvement, advocating for me throughout the project, and continuously steering me in the right direction. I would also like to thank my lab mates and friends, Keaton Coletti, Cody Langston, Ryan Romeo, Ben Morris, and Jesse Mullis who helped me through this experience with both laughter and genuine advice. I would like to give special acknowledgments to Cody Langston for his contributions to the image analysis software used for crack detection. Cody took the lead on writing the software and is the sole reason for its success. Cody’s contributions include: developing the preprocessing procedure, devising the crack detection routine used, and implementing repeat crack detection, denoising, and crack stitching procedures. I would also like to thank my wife and parents for their support in my decision to pursue graduate school. Finally, I acknowledge the friendship, uplifting energy, confidence, and kindness that I have received during this time. I thank my mentors and colleagues for their motivation, outstanding guidance, resourcefulness, knowledge, openness, and support throughout this journey.

Contents

List of Figures

List of Tables

Chapter 1

Introduction

Pecans (*Carya illinoinensis*) are one of the most valuable tree nut crops native to North America [1]. Tree nuts are edible kernels inside the seeds of trees [2]. More than 98% of the world's pecan production occurs in the southern United States and Mexico [3]. Pecans are valued for their flavor, health benefits, and use in baked goods [4–6]. In the United States alone, pecan production averaged 267 million pounds (roughly $459 million worth) of in-shell pecans per year from 2018 to 2022 [7].

Before commercial pecan farming, pecans were a staple for indigenous people in North America and it took nearly four centuries for the pecan to become a cultivated crop [8]. Once pecans became a cultivated crop, varieties were improved upon by grafting multiple existing varieties as early as 1810 [2]. These grafted pecan varieties are known as improved varieties, and most of the pecans commercially harvested are improved varieties [9].

The first pecan trees planted for commercial nut production were located in Bustamente, Mexico in the year 1911 and the trees used were estimated to be around 200 years old [8]. The first planting of pecan trees in Georgia dates back to 1830 when a barrel of pecans washed ashore from a shipwreck near Saint Mary's and the nuts from the barrel were planted in the ground [2]. Now, Georgia is the largest pecan producer in the United States [10].

Pecans are composed of a kernel surrounded by packing material and encased in a hard shell. It is common practice to crack the outer shell and separate it and the packing material from the kernel before sale to increase the price per pound [11]. Industrial pecan cracking and shelling equipment has been developed to process large amounts of harvested pecans.

In industrial processing, the pecan is impacted to crack the shell so it can be removed later [12]. A common method for mechanized pecan cracking involves orienting a single pecan on its end and striking it with an impacting die. This is known as end-to-end cracking [9]. The main objective during cracking is to apply enough force to thoroughly crack the outer shell without damaging the enclosed kernel. After the pecans are cracked, they are fed through a mechanized sheller to separate the shells from the kernels.

A typical pecan sheller consists of a rotating bar with smaller protruding rods (often called a "beater bar"), which is encased inside carefully spaced rotating rings [9]. The beater bar hits the cracked pecans to remove the shells. The spacing between each ring is tuned so that kernels can drop through the spaces while unshelled pecans remain in the sheller.

1.1 Motivation

During the cracking and shelling process, the pecan kernels are often broken or damaged [11]. Kernel damage is undesirable as intact kernels have an increased value per pound compared to pieces or meal [11]. New equipment and methods for cracking and shelling need to be tested and validated to minimize damage to the kernels during kernel extraction.

Not only is there a need for improved cracking and shelling equipment, but also means of quantifying the results of the equipment. Typically, when pecan cracking and shelling methods are considered, insufficient information is collected that can be used to evaluate a cracking or shelling method. For cracking, the most common metric studied is the rupture energy [13–17], but the type of cracks produced and how easily the kernel can be removed are rarely considered.

Rupture energy is often computed by pseudo-statically loading tree nuts. A rupture energy computed from pseudo-static loading may not be useful because impulsive forces are used to crack tree nuts in industrial processing. The failure point of a tree nut shell is strain-rate dependent, so only rupture energies computed for high strain rates may well inform tree nut processors.

Research that specifically considers crack types tends to generate measurements from visual inspection and tends to be imprecise or subjective [18–21]. There exists a need for a repeatable and accurate method to measure the efficacy of cracking procedures of pecans.

1.2 Outline and contributions

This thesis addresses the problem of kernel damage during industrial pecan cracking processes. The problem is addressed by first developing a data collection procedure for experimentally testing pecan cracking methods, then the data collection procedure is used to experimentally determine an improved impactor geometry for end-to-end pecan cracking.

The principal contributions of this work are summarized as:

1. Developing an image processing software for the detection, classification, and measurement (DCM) of pecan cracks;

2. Determining optimal impact energy and impactor geometry for end-to-end pecan cracking for ease of shelling and avoiding kernel damage.

Although crack detection is well-researched for some applications, detecting cracks in pecans poses unique challenges that other applications do not. For example, pecan shells are dark brown with dark spots, making it difficult to differentiate between shells and cracks. Addressing this challenge requires additional noise reduction and validation steps to differentiate cracks from dark spots. An additional challenge relates to the roughly ellipsoidal shape of pecans. The curvature of the pecan can have image-warping effects and also necessitates the acquisition of multiple images to map the entire surface area of the nut. To address the latter challenge, the image processing software (hereafter referred to as the DCM software) described in this thesis processes video files of rotating pecans to generate an accurate map of the entire pecan surface.

Another challenge is that pecan cracks can sometimes extend around the entire circumference of the pecan, resulting in cracks that do not have a clear beginning and end. The DCM software addresses these situations with a classification step determining how the crack should be measured. The final challenge is that if the video file captures the pecan rotating multiple times, multiple instances of the same crack are often detected. To address this issue, the DCM software compares the geometry of each detected crack and discards any cracks that are determined to be nonunique.

The problem of kernel damage during cracking is addressed by comparing the efficacy of different impactor geometries. The nuts are cracked across a range of energy levels for each impactor geometry, and the resulting cracks are divided into four categories. These categories are selected based on how easily the shell can be removed from the kernel. Cracks are categorized with the help of the DCM software. An optimal energy range is determined for each impactor geometry. The impactor geometries are then evaluated based on their ability to maximize the preferred crack types throughout the widest possible impact energy range.

Chapter 2

Background

2.1 Pecan processing and handling

Pecan cultivation begins in fields where pecans are grown on a long-lived tree species. Pecan moisture begins around 30% as the kernels develop and will drop to 8% as mature nuts begin to drop [2]. Once the nuts have ripened, they are forced to the ground by shaking the tree trunks with mechanical shakers. In some cases, individual limbs of pecan trees are shaken to remove mature nuts. The pecans can then be manually collected off the ground, swept into bins, or rolled into a hopper similar to how golf balls are collected on a driving range.

Once the nuts are collected, they are cleaned of dirt, sticks, leaves, clods, and remaining husks. The nuts are then graded through shaking screens to sort out broken nuts, unhulled nuts, and other various debris. After being cleaned and graded, they are sized from 10/16 (in.) to 15/16 (in.) in increments of 1/16 (in.) [6]. Once sized, they are dried to a moisture level of about 4.5% to remove the moisture of the sap which prevents discoloration, molding at the apex of the nut and the breakdown of oil [2]. Drying the nuts also shrinks the kernels, which prevents them from getting stuck inside the shells. Nut drying is typically done through blowing of atmospheric or refrigerated air.

After the nuts are dried and stored, moisture is re-introduced to the nuts before cracking and shelling. Introducing moisture into the nuts makes the kernels more ductile and less susceptible to damage during cracking and shelling [2].

A preliminary study is conducted to investigate the pecan conditioning time and its effect on the moisture of the kernel. Groups of five pecans are conditioned in a hot water bath at 100° C for five to 70 minutes and the moisture content of the kernels is determined. The moisture content is measured by drying the kernels at 100°C until they reach a constant weight. Any weight loss is reported as percent moisture [22]. The results of the moisture study are shown in Fig. 2.1. Each triangular marker is the average moisture of the five pecans tested per condition time. The moisture measured in each pecan is illustrated by the dots. The line shows the trend in average pecan moisture as a function of condition time.

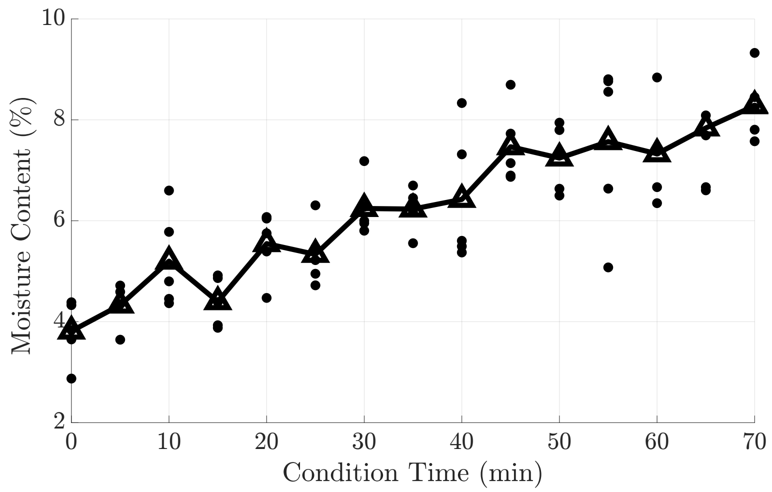

Figure 2.1. Pecan moisture level as a function of condition time in a hot bath at 100°C.

2.2 Tree nut cracking

Mechanized pecan shelling began in the 1920s as demand for the shelled nut increased. The first successful automatic cracker was designed by Lee J. Meyer of San Antonio, Texas [2]. The act of shelling reduces weight of the nuts by 64%, volume by 50% and storage life by 74% [2]. The amount of force required to crack the nuts is a function of shell thickness.

Previous research has studied the mechanical properties of various tree nuts to better prevent kernel damage during cracking and shelling [13, 16, 17, 23, 24]. Braga et al. [24] studied rupture energy for macadamia nuts as a function of moisture content, nut size, and loading orientation. Olaniyan et al. [16] studied the effect of temperature, loading orientation, and moisture on the rupture force of shea nuts. This work also defined toughness and firmness values for shea nuts by quasi-statically loading the nuts. Koyuncu et al. [17] conducted a similar study that analyzed the rupture energy of walnuts as a function of shell thickness, geometric mean diameter, and loading angle. Man et al. [15] validated a continuous damage theory by measuring the probability of breakage on walnuts. The damage theory was then used to determine the upper and lower bounds on the fracture energy of large subsets of walnuts.

For pecans, Kabas et al. [13] determined engineering properties such as strength and friction coefficient, toughness, and firmness as a function of the moisture of the kernel and the orientation of the load. They found that circumferentially loaded dry pecans had the lowest rupture energy; however, dry kernels are brittle and susceptible to damage during cracking [25], and most pecan processing equipment uses end-to-end cracking [26]. Celik et al. [27] created a material model for pecan shells and pecan packing material, which was then implemented in a dynamics package in a commercial finite element analysis software.

Another approach to research in industrial tree nut processing involves the experimental observation of the cracking and shelling processes of different tree nuts. Forbus et al. [11], Okunola et al. [28], Olaoya et al. [21], Oluwole et al. [19], and Prussia et al. [18] conducted experiments analyzing cracking efficiency with respect to moisture content of different tree nuts. Although controlling moisture aids in the processing of tree nuts in industrial settings, the issue of kernel damage persists. Okunola et al. [28], Olaoye et al. [21], and Oluwole et al. [19] conducted larger-scale experiments using industrial tree nut processing equipment. In these studies, various settings of the cracking equipment are changed, and the cracking efficiencies are compared for each setting.

2.3 Crack detection

Crack detection involves identifying cracks in a structure of interest using techniques such as acoustic, thermal, laser, radiographic, and machine vision [29]. Machine vision is becoming increasingly popular due to its non-destructive nature and ease of data collection [29]. Most crack detection algorithms that use machine vision follow a similar sequence, including image acquisition, preprocessing, image processing, crack detection, and parameter estimation [29]. This sequence of steps can be adjusted depending on the surface geometries, crack shapes, background noise, and camera settings [30].

Two popular strategies used for crack detection are thresholding and edge detection. The thresholding strategy assumes that pixels corresponding to cracks have different color values than their counterparts. Thus, pixels with a color value in a specified range are assumed to correspond to cracks [30]. The edge detection strategy assumes that crack edges are represented as sharp changes in color values in the image. Edge detection strategies use matrix decomposition to detect discontinuities between relatively continuous regions in the image [30].

One primary application of crack detection is in the processing of eggs because the presence of small cracks in the shell of an egg can lead to bacterial contamination [31]. Since any size crack can result in contamination, the priority in this application is to detect cracks rather than measure them. A setup commonly used for egg crack detection involves placing the eggs in a vacuum chamber, illuminating them from below, and comparing the pictures taken at atmospheric and vacuum pressures [32]. The vacuum chamber setup has been improved to detect microcracks and dirt in unwashed eggs using different edge detection algorithms with reported accuracies ranging from 94% to 100% [31, 33].

Civil infrastructure health monitoring has been another driver for improvements in crack detection algorithms because increasing the accuracy of inspections can prevent catastrophic failures [34]. Since crack sizes can be used as indicators of structural degradation, crack detection in this application is concerned with both detection and measurement. Previous work has investigated edge detection methods by Roberts, Sobel, Prewitt, Gauss-Laplacian, Canny, and Gabor with a percentage of accurately classified pixels ranging from 70.2% to 77.7% [35, 36]. Other studies have focused on accurately measuring cracks in civil infrastructure. Crack width measurements have been reported with accuracies of 94% to 97.9% [35, 37]. Surface mapping has also been used to automate crack detection using robotic trucks and drones. This approach has been shown to measure the lengths of the cracks with accuracies of 70% to 91% [38, 39].

Chapter 3

An image processing method for the detection, classification and measurement of pecan cracks

Much of the content in this chapter is obtained directly from the author's research article currently in review [40].

3.1 Materials and Methods

For this research, the McMillan variety of pecans were sourced from an orchard in Athens, Georgia (USA). The pecans are cleaned by the harvester and then dried for storage. Before storage, a small subset of dried pecans is cracked and shelled, and the moisture content of the kernel is found to be 3.8%. Throughout this study, the moisture content is measured by drying the kernels at 100^oC until they reach a constant weight. Any weight loss during drying is assumed to be evaporated moisture [41].

After drying, the remaining in-shell pecans are stored in a freezer to preserve freshness and prevent the onset of rancidity [6]. Sets of pecans are removed from the freezer as needed for cracking and image analysis. A total of 410 pecans are separated into two sets. The first set of 300 pecans is conditioned by a hot water bath in a process that consistently produces a kernel moisture content of approximately 8%. The second set of 110 pecans is not conditioned and is cracked at the storage moisture content of 3.8%.

3.1.1 Cracking procedure

Two sets of cracked pecans are produced using three cracking methods. The first set comprises 30 pecans cracked using a gravity-based drop tower at 3.8% kernel moisture. Pecans cracked by this method show a more diverse set of cracks, making this set ideal for calibration. For validation, a second set of 380 pecans is cracked using two industry-standard crackers. The first cracker is the ME-JC-24 cracker (Modern Equipment & Electronics). This loads the pecans along their circumference as they roll between two compression plates. The second cracker, the ME-MC cracker (Modern Equipment & Electronics), applies an axial compressive load to one pecan at a time. Of the 380 pecans cracked with industrial crackers, 300 are conditioned to a kernel moisture content of approximately 8%. To generate a more diverse set of crack geometries, 80 additional pecans at 3.8% kernel moisture are cracked (40 in each cracker) and added to the validation set. Sometimes, pecans become pulverized during cracking, leaving the kernel heavily damaged. Any pulverized pecans are omitted from the study and not included in the calibration or validation sets.

3.1.2 Video acquisition setup

Fig. 3.1a shows the video acquisition rig designed and built to enable a consistent method of collecting videos of rotating pecans. This rig is 76.2 x 47 x 20.3 cm in size and is painted white to contrast the pecans and their background. The rig comprises two 3.18 cm diameter PVC rollers, positioned 5 cm apart. A pecan is placed between the two PVC rollers, as seen in Fig. 3.1b. The pecan rotates with the PVC rollers, allowing for a full view of the pecan. One of the rollers has three 0.32 cm tall ridges equally spaced along the azimuth to prevent pecans from getting stuck. The rig is driven by an 18 W motor that rotates both wheels at a constant speed of 30 rpm. Four 5000 Kelvin lights are mounted to the rig to illuminate the pecans.

A GoPro Hero 8 camera captures video at 2704 x 1520 resolution and 60 frames per second. The default camera settings are adjusted to a white balance of 6500 Kelvin, an ISO of 6400, and a digital zoom of 1.4x. The camera is mounted 25.4 cm directly above the rollers using a three-arm mount, as seen in Fig. 3.1a. This mounting distance is the minimum required for the pecans to remain in focus with the GoPro's 19-39 mm linear lens. The pecans are placed in the center of the frame and the video files are acquired by placing a pecan on the rig, turning the motor on, and capturing four seconds of video on the GoPro. This video is then transferred to a computer using GoPro's USB interface.

(a) (b)

Figure 3.1. (a) Video acquisition setup and (b) pecan placement in the rig.

3.1.3 DCM software overview

The DCM software is developed using MATLAB 2023a and its library of existing image and video processing tools. Fig. 3.2 shows the sequence of steps performed by the software, including the four main steps of preprocessing, crack detection, crack classification, and crack measurement. Pre-processing encompasses segmentation, masking, rotation, and video reassembly. These pre-processing steps are performed to reduce the data size and initialize the video for crack detection. Crack detection uses a thresholding strategy and is adjusted to work with video by introducing crack stitching and repeat crack detection steps. The crack stitching step accounts for the pecan's rotation between frames, while the repeat crack detection step accounts for the possibility of detecting non-unique cracks. After detection, the DCM software assigns a classification to each unique crack and performs a measurement corresponding to that classification.

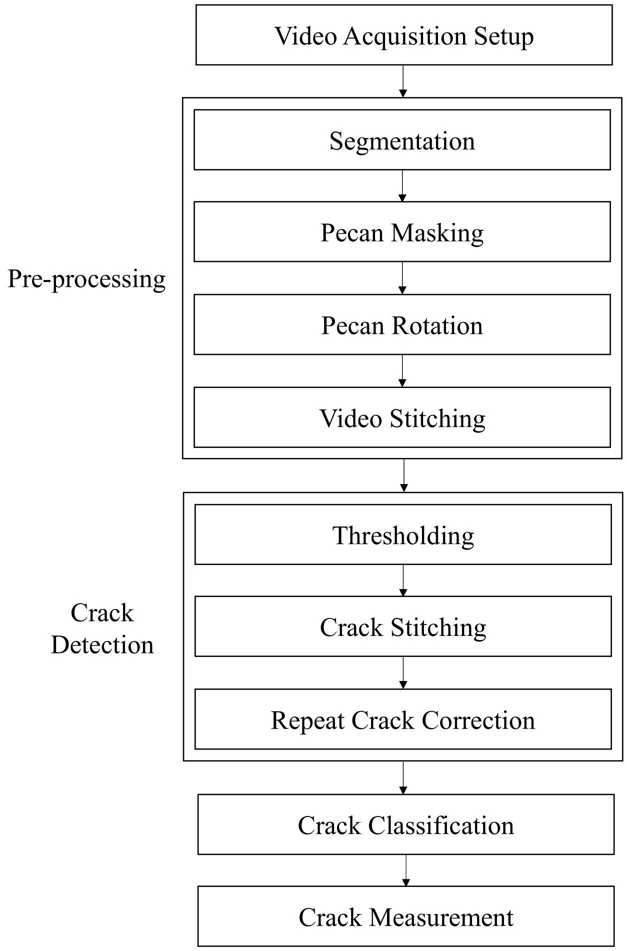

Figure 3.2. Video processing structure for parameter estimation.

3.1.4 Pre-processing

The video is first segmented into two second intervals for memory management. The segments are then converted from an RGB (red, green, and blue) colorspace to an HSV (hue, saturation, and value) colorspace, and the red and saturation values are stored as shown in Fig. 3.3a. Pecans are isolated from the background by thresholding the saturation map for values between 0.35 and 1. Fig. 3.3b shows the resulting binary large object (known as a "blob") corresponding to the isolated pecan. The DCM software then fits an ellipse to each blob to calculate the long-axis orientation. The isolated pecan blob is rotated so that its long axis points vertically. This rotated blob is cropped and multiplied by its corresponding saturation and red values, resulting in a rotated saturation map like the one shown in Fig. 3.3c. This rotation accounts for changes in the yaw angle of the pecans as they rotate. Once the entire video is processed, the two second segments of cropped red and saturation values corresponding to the pecan are stitched chronologically.

3.1.5 Crack detection

When a complete video of a pecan is stored, it is sent through the crack detection strategy shown graphically in Fig. 3.3d. The crack detection strategy thresholds the saturation values since cracks and pecan kernels have higher average saturation values than the surrounding shells. The DCM software starts by generating a histogram of the saturation values ranging from 0 to 255 with a bin width of one. The absolute maximum of this histogram is stored and a nearby minimum is then found by searching the 32 bins above the maximum value. This minimum is a local minimum if and only if the frames containing cracks follow a bimodal distribution, as shown in Fig. 3.4b. This bimodal distribution has two peak values, one corresponding to the mean saturation value of the pecan shell and another corresponding to the mean saturation value of the pecan cracks and exposed kernels. If a local minimum between the two peaks is detected, the saturation map is thresholded at the value corresponding to the local minimum. This thresholding considers all pixels with saturation values above the local minimum as cracks.

Fig. 3.4a shows a case where no local minimum is found; therefore, no cracks are detected. If the location of the absolute maximum is higher than a value of 167, the saturation map is thresholded at 167 instead of the local minimum. An absolute maximum above 167 suggests that the kernel is in most of the frame, resulting in the distribution shown in Fig. 3.4c. The bin width, search bounds, and kernel saturation values are calibrated using the calibration procedure discussed in Section 3.1.10.

The binary frames with detected cracks are cleaned using a strel method to remove noise and connect disconnected clusters of pixels that are part of the same crack. The strel method includes a dilation step to help connect nearby clusters of pixels. The dilated image is then eroded to remove pixels on the boundary of the newly connected pixel clusters. Here, images are dilated by five pixels and eroded by four. As a de-noising step, identified cracks that are less than 200 total pixels are assumed to be false positives and are not considered for classification and measurement.

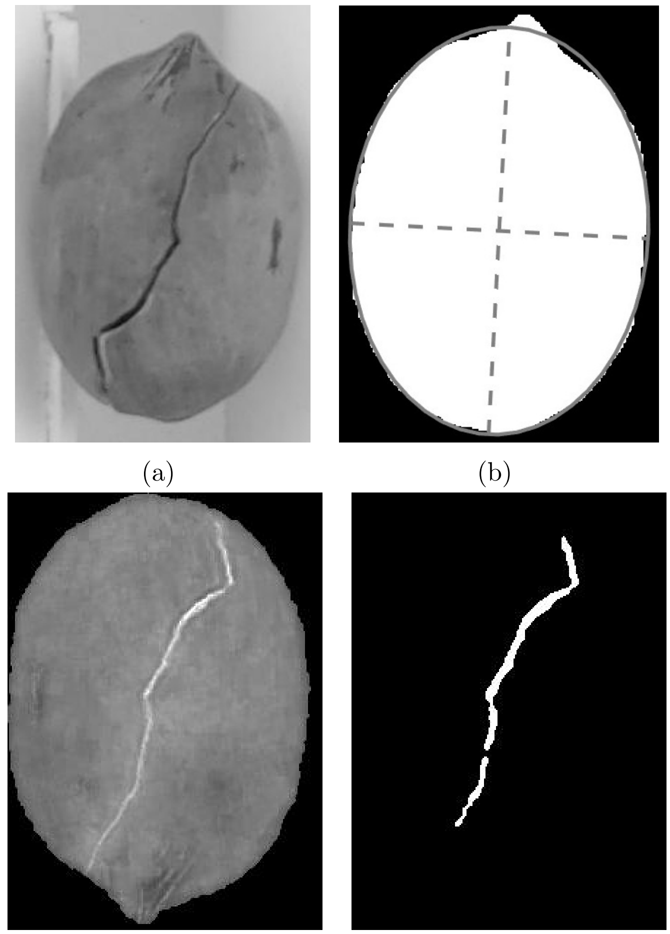

(a) (b)

(c) (d)

Figure 3.3. Crack detection method for (a) saturation image, (b) binary mask, (c) rotated saturation mask, and (d) thresholded binary crack.

3.1.6 Crack stitching

After the cracks are detected for each frame of the video, they are connected to cracks identified in adjacent frames using a process known as stitching. The DCM software uses KAZE feature detection to find and match unique features in two adjacent frames and then calculate an average translation between the two frames. A complete review of KAZE feature detection is detailed in Ref. [42]. This feature detection is performed on the saturation and red values of the pecans, as shown in Fig. 3.5a. The DCM software uses the five features closest to the frame's center to bias the stitching towards areas that are viewed head-on. The average translation between frames is calculated without rotation, change in scale, or warpage to preserve the geometry of the cracks. The DCM software uses the translation calculations to add the cracks together and ultimately generates

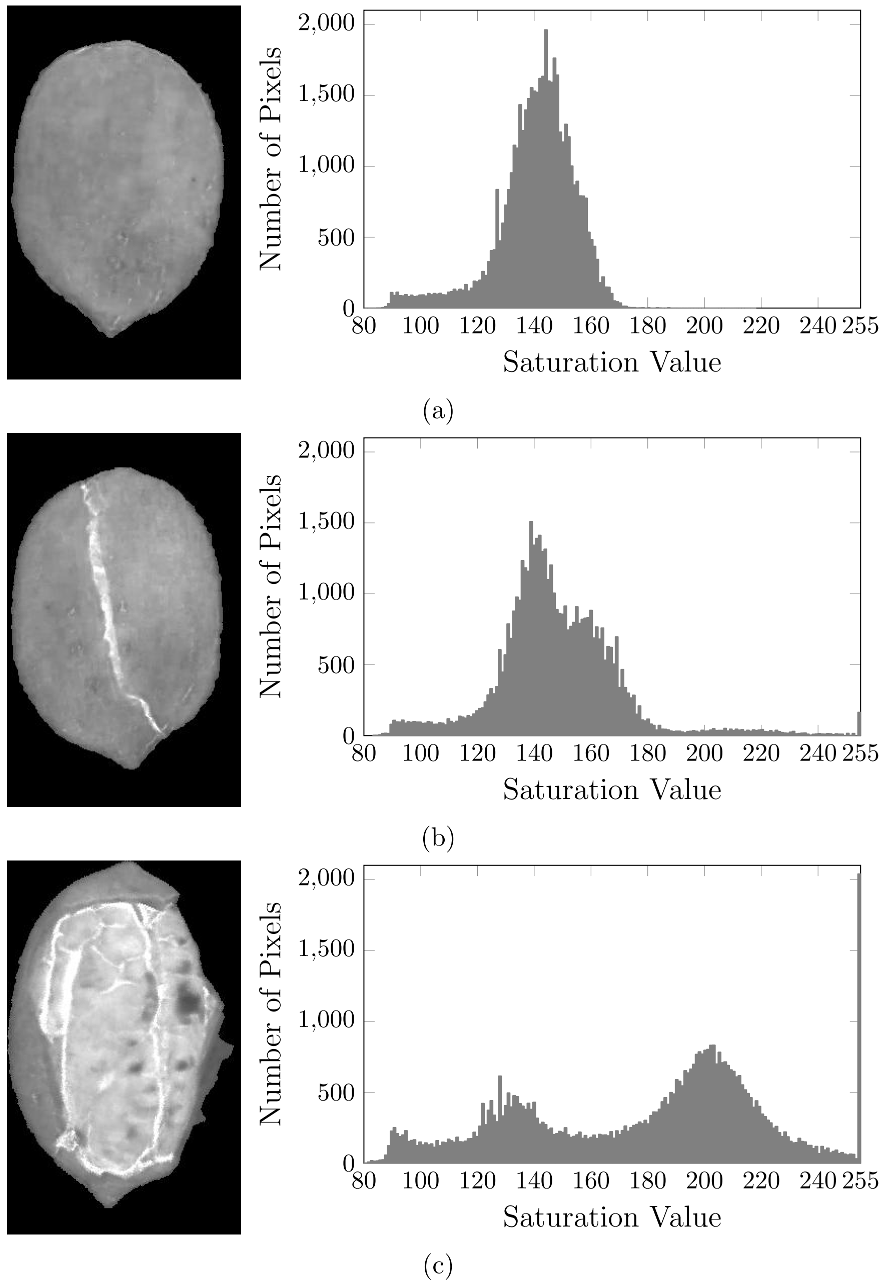

Figure 3.4. Saturation histogram for (a) uncracked, (b) cracked, and (c) open pecans.

a complete map of the cracks in the pecan shell, as seen in Fig. 3.5b. During stitching, the outer 20% of the pixels on both sides of each frame is removed because these surfaces are warped due to the curvature of the pecan. The DCM software also removes portions of the stitched crack map not represented in three or more frames to account for lighting anomalies. Cracks appearing only in the first or last few video frames are also removed as they are unlikely to be accurately represented.

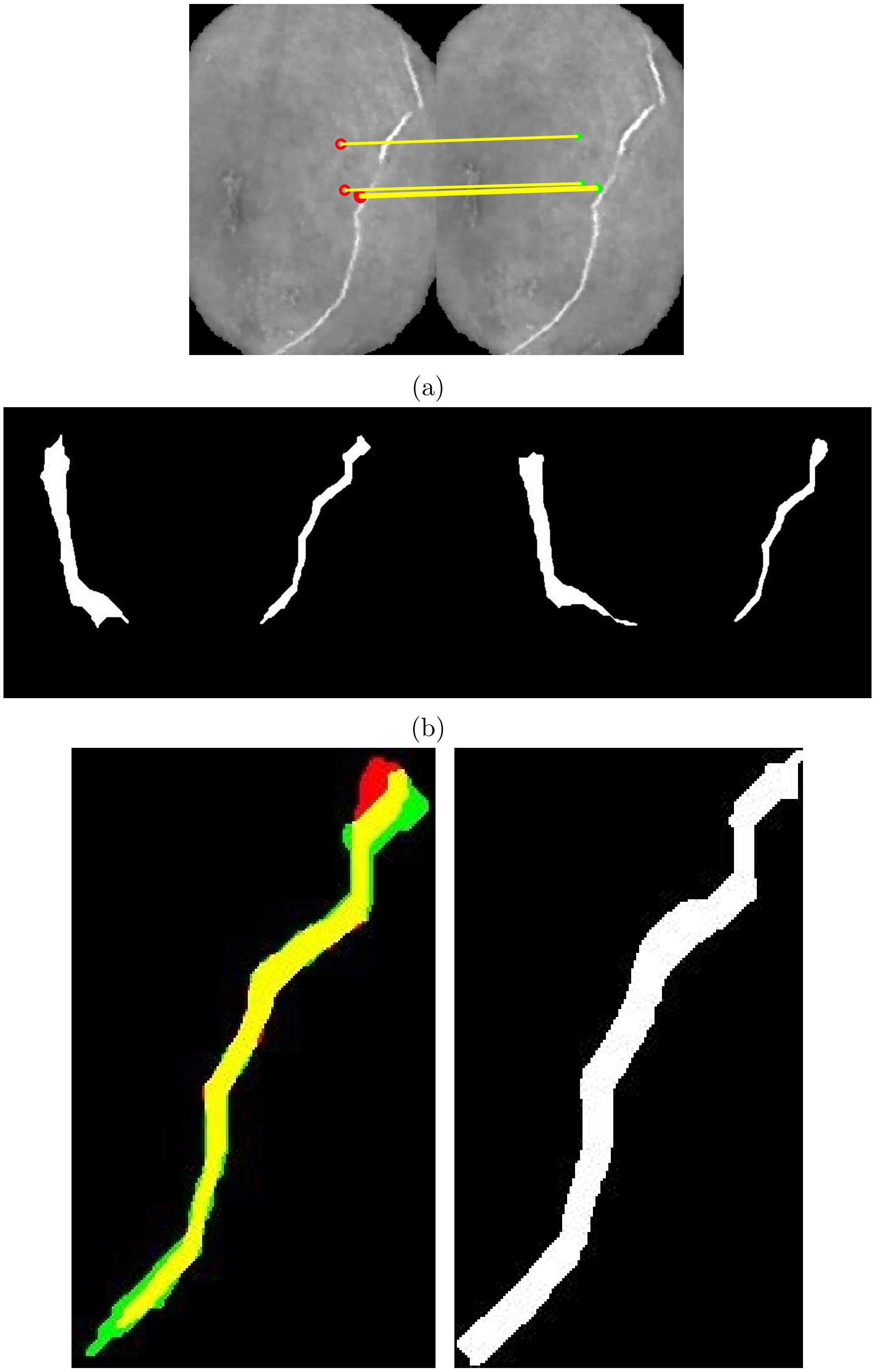

(a)

(b)

(c) (d)

Figure 3.5. Video stitching method for (a) KAZE feature detection, (b) binary crack map, (c) repeat crack detection, and (d) binary crack geometry.

3.1.7 Repeat crack detection

The pecans are typically rotated multiple times during each video. Consequently, the resulting crack map will consist of multiple images of the same crack. The DCM software accounts for this by performing a two-dimensional cross-correlation between each crack, which calculates the translational offset that results in the highest overlap, as shown in Fig. 3.5c. The DCM software computes the ratio of overlap area to crack area for each crack. If either of these ratios exceeds a threshold of 0.6 or the average of the two ratios exceeds 0.45, the binary cracks are considered the same and are labeled accordingly. The DCM software stores the largest crack by pixel area as the most accurate representation. An example of a stored crack is shown in Fig. 3.5d.

3.1.8 Crack classification

Cracked pecans are classified into the following crack types: longitudinal, circumferential, and open. The crack in Fig. 3.6a is an example of a longitudinal crack because the crack is primarily aligned with the long axis of the pecan. The longitudinal classification is the default classification. Alternatively, if the crack is primarily aligned with the short axis of the pecan, it is classified as circumferential (see Fig. 3.6b). The DCM software identifies circumferential cracks by comparing the crack length with the length of the pecan's circumference at the location of the crack. This identifies cracks that go around the entire circumference and connect to themselves and classifies them as circumferential. If a crack does not connect to itself, the angle the crack makes with the pecan's short axis is measured. If this angle is less than 30 degrees, the crack is also classified as circumferential.

An example of an open crack is shown in Fig. 3.6c. Open cracks are characterized as having a relatively large area of exposed kernel. Here, the software classifies cracks as open if the length-to-width ratio of the crack's bounding box is greater than 1:2 and the crack area takes up at least 40% of the bounding box area.

3.1.9 Crack measurement

The software's crack detection sub-process outputs an image representation for every unique crack on the pecan's surface. The crack images are classified, and measurements corresponding to the classification are taken. The end-to-end length of the crack is measured if the crack is classified as longitudinal. The software calculates this length by tracing the boundary of the crack to compute the largest Euclidean distance between pixels on this boundary with a resolution of 0.1 mm, as shown in Fig. 3.7a.

(a) (b) (c)

Figure 3.6. Example of (a) longitudinal, (b) circumferential, and (c) open crack.

For circumferential cracks extending around the entire shell, the pecan's diameter at the crack's location is measured to the nearest 0.1 mm to quantify the size of the crack. Since the cross-sections of pecans are not perfectly circular, a pecan's diameter at the crack's location varies slightly with azimuthal angle. The maximum diameter across all frames is stored as the diameter of the crack (see 3.7b). The crack area is measured for open cracks by summing the total number of white pixels in the binary image as shown in Fig. 3.7c. The area measurement has a resolution of 0.01 mm^2.

3.1.10 Software calibration and validation

A set of 30 pecans is used to calibrate the software. Each pecan in this set has a single crack. These cracks are manually classified by visual inspection, and the calibration set is configured to consist of ten longitudinal, ten circumferential, and ten open cracks. The calibration set is then used to set the threshold values, classification techniques, and noise reduction strategies for the DCM software. These cracks are chosen to represent different edge cases expected when cracking pecans and are not used for accuracy or precision studies.

The software's detection, classification, and measurement capabilities are validated on 380 pecans. The crack detection is validated by counting the number of times the software fails to detect a crack that is visible to the human eye, detects noise as a crack, or detects the same crack multiple times. Validation of the software's classification capability involves counting the instances in which the algorithm incorrectly classifies cracks relative to how a human classifies them.

To validate the measurements of the DCM software, the ground truth measurements are made manually on a set of 380 pecans. The lengths of longitudinal cracks are recorded by tracing the longest end-to-end distance on the crack boundary with a string, as shown in Fig. 3.8a. The string is then marked and measured with a ruler to the nearest mm. For circumferential cracks, the largest diameter is measured with calipers to the nearest 0.1 mm at the location of the crack, as shown in Fig. 3.8b. The area of open cracks is calculated by cutting a piece of lead tape to the shape of the crack and weighing it on a scale to the nearest 0.01 g which corresponds to an area measurement resolution of 50 mm^2 (see Fig. 3.8c). The measurement accuracy of the software is then calculated by comparing the manual measurements to the software output rounded to the manual measurement resolution.

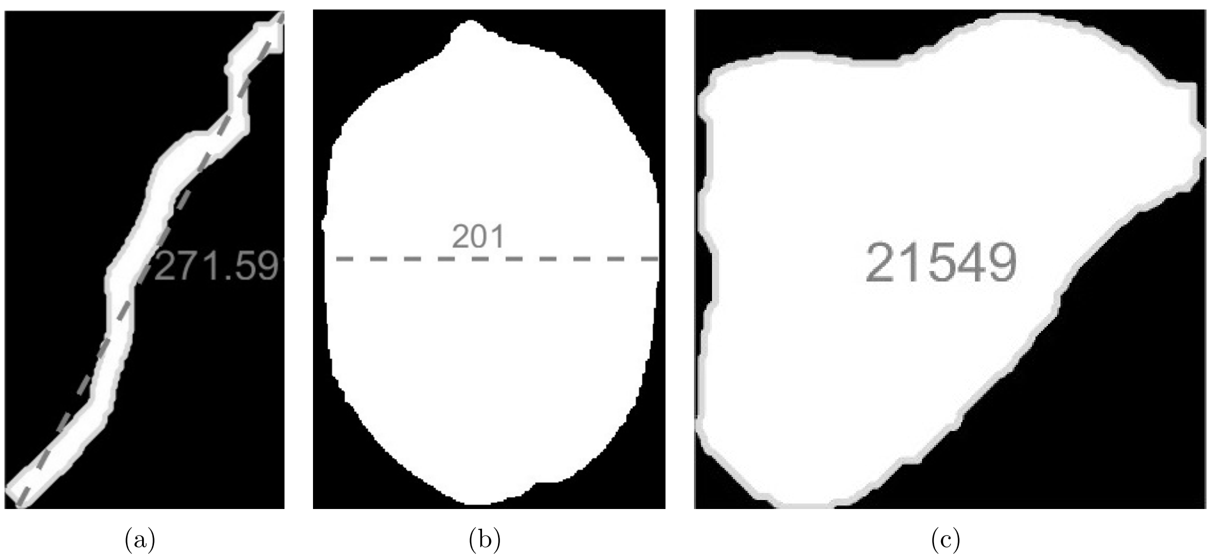

Figure 3.7. Computer measurements of (a) longitudinal length, (b) circumferential diameter, and (c) open area.

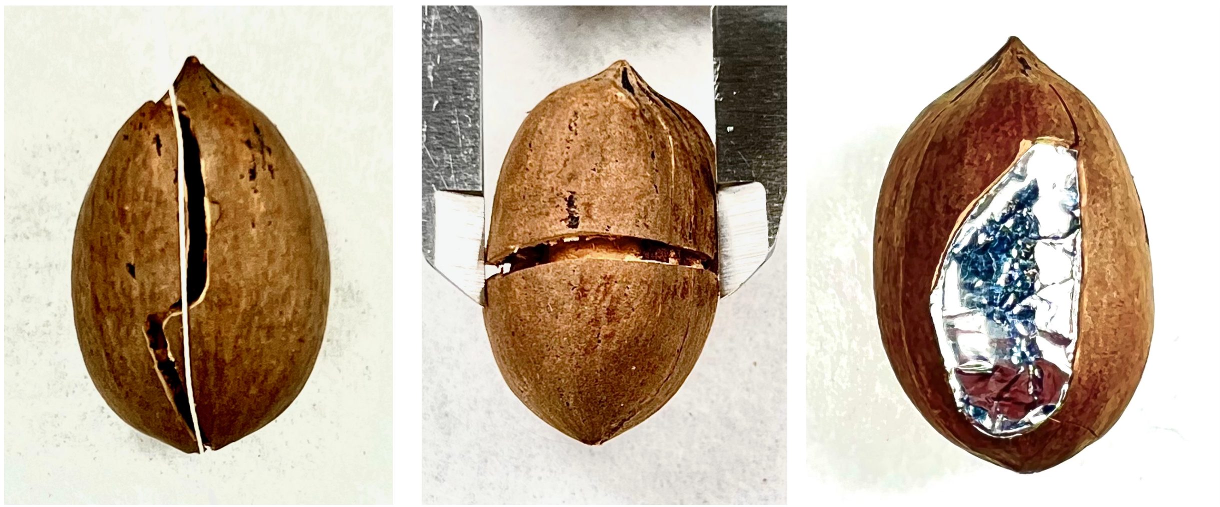

(a) (b) (c)

Figure 3.8. Manual measurement of (a) longitudinal crack length by measuring the length of a string connecting crack endpoints, (b) circumferential diameter using calipers, and (c) open crack by filling in the crack with lead tape and subsequently weighing the tape.

3.2 Results and Discussion

3.2.1 Crack detection accuracy

As shown in Table 3.1, cracks are not detected on 34 of the 380 pecans in the validation set, which corresponds to a 91% detection accuracy. Of the cracks that are not detected, 15 are longitudinal and 19 are circumferential. All 36 open cracks and 60 uncracked pecans are accurately detected. Open cracks are consistently detected due to their size and presence in a large portion of the frames captured. The DCM software consistently prevents false positives due to the lighting and noise reduction steps that prevent pecan dark spots from being identified as cracks.

Most of the cracks not detected by the software can be classified as micro-cracks. Here, micro-cracks are defined as cracks that do not penetrate the entire shell thickness and have a maximum thickness of less than 0.4 mm. The validation set includes 41 micro-cracks, which accounted for 12 of the longitudinal and 13 of the circumferential crack detection failures. In general, the circumferential and longitudinal micro-cracks have a detection rate of 23.5% and 50%, respectively. The DCM software has a higher detection rate for longitudinal micro-cracks since the azimuthal rotation of the pecans allows this type of crack to be viewed from multiple angles.

The remaining nine crack detection errors are caused by poor camera orientation and crack placement. The camera cannot view cracks residing entirely near one end of the pecan. A dual-camera setup is tested on a subset of 100 pecans in an attempt to fix this issue. The dual camera setup is found to reduce detection errors by 50% but suffers from reduced measurement accuracy. The decrease in measurement accuracy is due to the foreshortening of cracks since the setup requires that the pecans be viewed obliquely. Despite improving detection, the dual camera setup has not been pursued further, since it doubled the software runtime and reduced the accuracy of measurements.

3.2.2 Crack classification and measurement accuracy

The validation set resulted in the distribution of crack types shown in Table 3.1. The classification algorithm has an overall accuracy of 98.7% as only five pecans are misclassified due to misrepresentating crack geometry. In all five cases, misclassification occurs because a small portion of the two ends (*i.e.*, the poles) are out of the camera's view. In these cases, a single circumferential crack traversing an end is classified as two separate longitudinal cracks.

Table 3.1 shows the accuracy of the software's measurements relative to the manual measurement. The measurement accuracy for longitudinal, circumferential, and open cracks are 91.5%, 95.4%, and 92.8%, respectively. The measurements for circumferential cracks have the highest accuracy because the diameter measurements have a low sensitivity to noise and curvature. Measurements for open cracks have lower accuracy since crack stitching accounts for in-plane translation without rotation, scale change, or warpage. Without these considerations, the edges of the representation of the open crack are less defined, which artificially inflates area measurements. Longitudinal cracks have the lowest accuracy, as their measurements have a high sensitivity to warpage and noise. Warpage is introduced when projecting the curved surface of the pecan onto a two-dimensional map. The increased curvature at the top and bottom of the pecan results in the representations of longitudinal cracks curving toward the long axis, which artificially increases the software's length measurement of the longitudinal cracks.

	Classification Distribution			Software Accuracy		
Crack Types	Conditioned	Dry	Overall	Detection	Classification	Measurements
Longitudinal	113	22	135	118/135	115/118	91.5%
Circumferential	122	30	152	133/152	131/133	95.4%
Open	16	20	36	36/36	36/36	92.8%
Uncracked	52	8	60	60/60	60/60	–

Table 3.1. Detection, classification, and measurement accuracies of cracked pecans.

3.3 Conclusions

Manually measuring cracks in pecan shells can be difficult, time consuming, subjective, and generally impractical in research and industrial settings. In this study, a software package is developed to automatically detect, classify, and measure pecan cracks using videos of rotating pecans. The software detected 90.6% of cracks, correctly classified 98.7% of detected cracks, and resulted in measurement accuracies from 91.5% to 95.4%. Future work will use the software to investigate how crack geometry affects the ease with which the shell can be liberated from the kernel. In addition, the software can be combined with cracker feedback control to generate cracks that enable easy shelling while limiting kernel damage.

Chapter 4

The effect of impactor geometry on end-to-end pecan cracking

Much of the content in this chapter is obtained directly from the author's research article [43].

4.1 Materials and methods

This study is designed to consider the end-to-end cracking of pecans. The impactor geometries are varied by changing their internal angle, as shown in Figure 4.1 by the angle θ. The impactors are manufactured from steel, which is consistent with industrial impactors. A total of four impactors are designed with internal angles varying from $30.0°$ to $52.5°$ with incremental steps of $7.5°$. The center of the impactor is drilled out to allow for proper seating of the pecan in the impactor.

The different impactor geometries contact different portions of the pecans as they rest inside the impactor. For example, the lowest angle impactor ($\theta = 30.0°$) contacts the pecan closest to its middle while the largest angle impactor ($\theta = 52.5°$) contacts the pecan closest to its end. Pecans are cracked at a range of energy levels and the crack types are measured and recorded. Once an energy threshold is reached such that every impact results in kernel damage, the experiment is terminated.

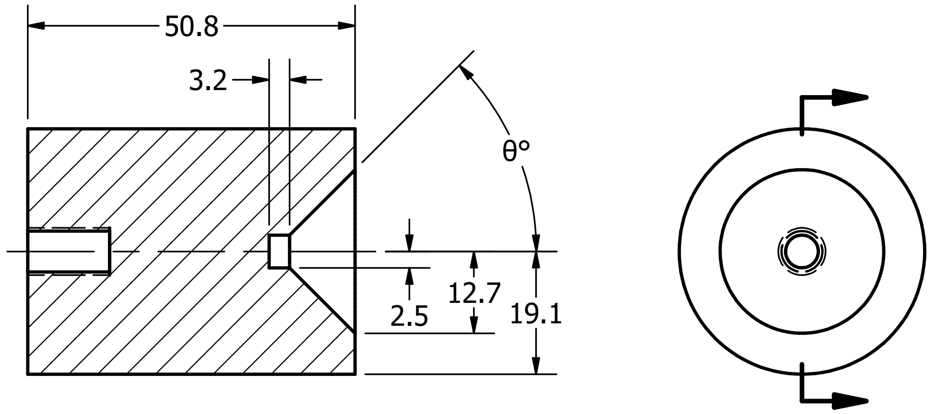

Figure 4.1. Dimensioned schematic (mm) of pecan impactor with specified impactor angle, $\theta°$.

4.1.1 Pecan processing and conditioning

In this study, pecans of the McMillan cultivar are obtained from a farm in Athens, Georgia (USA). McMillan pecans are of average quality and have thick shells with a high level of production and good pest resistance [44]. The thick shell makes them ideal for a pecan cracking study, as thicker shelled pecans require more energy for rupture [2]. Fresh pecans are used for this research from the harvest seasons of 2022 and 2023. Once harvested, the pecans are dried to a moisture level of approximately 4% and stored in a freezer to preserve their freshness and prevent the onset of rancidity [6]. Before testing, the pecans are removed from the freezer in batches ranging from 150 to 300. The pecans are conditioned with a hot water bath at a kernel moisture of approximately 8%. This relatively high moisture level makes the kernels more ductile and less susceptible to damage during cracking and shelling [2].

4.1.2 Drop weight rig design

The cracking force is controlled using the drop weight rig shown in Figure 4.2a. A pecan is placed between two static impactors and a falling weight of known mass (nominally 1.5 kg) is raised and dropped on the impactors, as shown in Figure 4.2b. The rig consists of a 45.5 x 45.5 x 5.0 (cm^3) aluminum base with a 1.2 (m) clear PVC pipe mounted 11 cm above the base. The PVC pipe acts as a guide for the drop weight. Affixed to the PVC pipe is a measuring tape to measure the height of the weight before it is dropped. A string tied to an eye bolt at the top of the weight is used to raise it to the desired height. A pulley is mounted on the top of the PVC pipe to guide the string.

To contain the shattered pecan shells, an acrylic shield surrounds the area where the pecans are cracked.

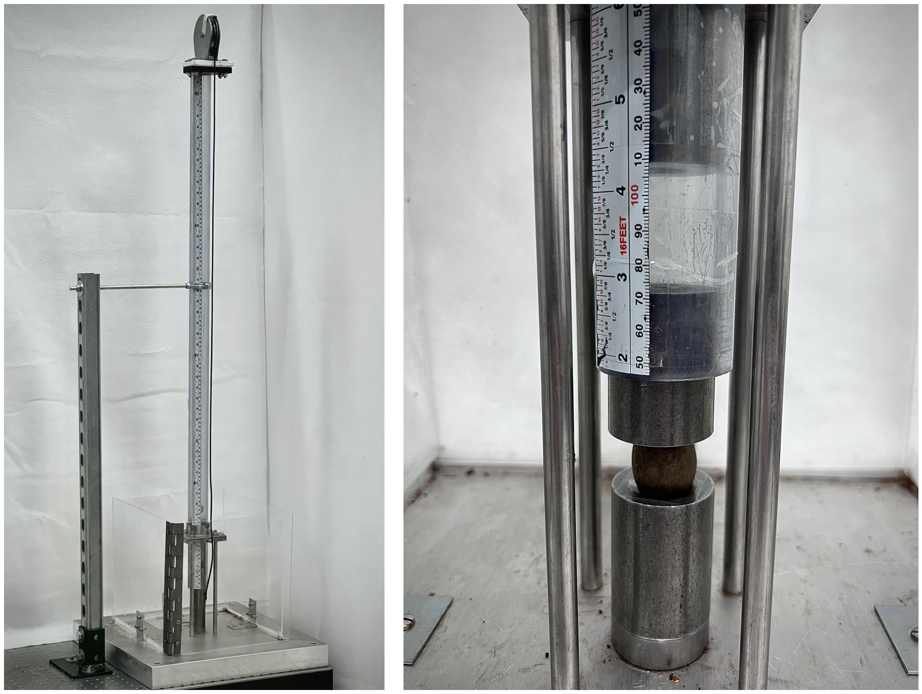

(a) (b)

Figure 4.2. (a) Cracking drop weight rig used in experiments and (b) placement of pecan in the rig.

During data collection, underdeveloped and diseased pecans are discarded, and a pecan is re-cracked in its place. Since the pecans are placed upright on the impactors, dust from the shells would collect in the impactors and be periodically cleaned to ensure that the pecans fully seat in the bottom impactor. In the case of the 30° impactor, nuts are occasionally forced into an impactor and become stuck after impact. Smaller pecans would get stuck more often, which implies that impactors should be sized down to avoid this problem. Should the 30° impactor be used in an industrial setting, impactors may need to be sized according to the size of the pecans being cracked.

4.1.3 Experimental parameters

The four different impactor geometries tested are shown in Figure 4.3. The gravitational potential energy ($E = mgh$) is computed for each drop height and used as the measure of the impactor energy. Here, E is the impact energy, m is the mass of the drop weight, g is the gravitational constant (9.81 m/s^2), and h is the height of the drop. The energy range from 1.6 to 14.9 J is divided into 35 equally spaced bins. For each of the 35 bins, 20 impact energies are randomly sampled to be used as test points. The corresponding height of the drop weight is calculated for each test point and a pecan is impacted at each drop height.

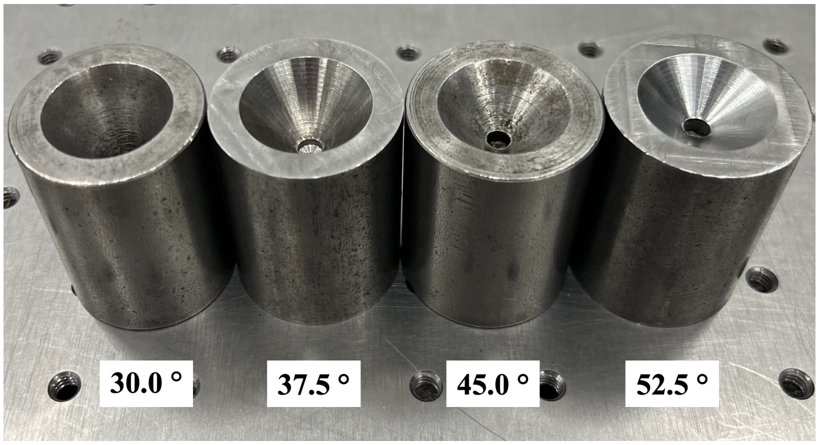

Figure 4.3. The four impactor geometries considered for pecan cracking.

To verify that impactor potential energy is an appropriate metric with which to study cracking trends, a sub-experiment is conducted. In this sub-experiment, the drop weight and drop heights are varied while maintaining the same potential energy. Drop weights with masses of 1.0, 1.5, and 2.0 kg are considered. Throughout the sub-experiment, the industry standard 45° impactor is used [45].

4.1.4 Experimental cracker evaluation

After cracking, each pecan is classified according to the extent of its cracks. The four classifications are: under crack, standard crack, ideal crack, and over crack. Representative photos of pecans falling into each of these categories are shown in Figure 4.4. These categories are defined on the basis of how easily the shell can be removed. For cracks in which the shell remains mostly intact, shell removal is difficult and these pecans are deemed to be under cracked. Conversely, cracks with visibly damaged kernels are said to be over cracked. Pecan cracks with easily removable shells and undamaged kernels are classified as standard or ideal cracks. Ideal cracks are differentiated from standard cracks by the entire circumference of the pecan being cracked so that the shell practically falls away and the kernels can be easily removed.

(a) (b) (c) (d)

Figure 4.4. Pecan cracks classified as (a) under crack, (b) standard crack, (c) ideal crack, and (d) over crack.

Separating the upper and lower halves of the pecan shell is found to be the easiest way to remove the kernels without damaging them. A cracked pecan is labeled as under cracked as shown in Figure 4.4a if the crack present extends less than 40% around the circumference of the pecan. This category also includes pecans that do not have visible cracks after being impacted. The 40% threshold is used because it is observed that if more than half of the circumference is intact, separating the top portion of the shell from the bottom is more difficult and requires more force than if more than half the circumference of the pecan is cracked. For standard cracks, as seen in Figure 4.4b, a circumferential crack extends across more than 40% but less than 100% of the circumference of the pecan.

For ideally cracked pecans like the one shown in Figure 4.4c, the entire circumference of the pecan shell is cracked, making two distinct halves of the pecan shell that can be easily pulled apart. Finally, Figure 4.4d shows an over cracked pecan where the kernel is damaged. For each individual pecan tested, categorization is first performed by visual inspection, which identifies ideally cracked and over cracked pecans. To distinguish the under cracked pecans from standard cracked pecans, the DCM software evaluates the circumferential length of the cracks.

4.2 Results and Discussion

Table 4.1 shows the results for each of the four impactor geometries. A total of seven energy ranges are displayed, each of which contains five energy bins. In the lowest energy range, as the impactor

Impactor Angle	Crack Type	Energy range (J)						
		1.6 - 3.4	3.5 - 5.3	5.4 - 7.2	7.3 - 9.2	9.3 - 11.1	11.2 - 13.0	13.1 - 14.9
30.0°	Under	100%	64%	12%	4%	0%	0%	0%
	Standard	0%	23%	25%	5%	0%	0%	0%
	Ideal	0%	13%	62%	71%	51%	5%	0%
	Over	0%	0%	1%	20%	49%	95%	100%
37.5°	Under	92%	29%	7%	0%	0%	–	–
	Standard	8%	46%	18%	3%	0%	–	–
	Ideal	0%	24%	58%	26%	0%	–	–
	Over	0%	1%	17%	71%	100%	–	–
45.0°	Under	61%	8%	1%	0%	–	–	–
	Standard	33%	30%	1%	0%	–	–	–
	Ideal	6%	50%	21%	0%	–	–	–
	Over	0%	12%	77%	100%	–	–	–
52.5°	Under	41%	0%	0%	0%	–	–	–
	Standard	39%	7%	0%	0%	–	–	–
	Ideal	20%	51%	1%	0%	–	–	–
	Over	0%	42%	99%	100%	–	–	–

Table 4.1. Percentage of each crack type reported in seven energy ranges for each impactor geometry.

angle increases, the number of under cracked pecans decreases. Following this trend, the 52.5° impactor is the first to over crack 100% of the pecans with respect to energy, while the 30.0° is the last to over crack 100% of the pecans. This implies that on average, the lower the impactor angle, the more energy is required for cracking.

Intuitively, the lower energy ranges produce more under cracked pecans. Furthermore, as the energy level increases, more pecan kernels are damaged. For processability, standard and ideal cracks are preferred, while under cracked and over cracked pecans are not. Thus, the data in Table 4.1 are presented to easily observe the number of standard and ideal cracks produced for each impactor geometry. An important metric is the energy level that maximizes the number of standard and ideal cracks. However, since the energy level in industrial pecan cracking equipment can only be crudely adjusted, a perhaps more important metric is the extent of the energy range over which a high percentage of standard and ideal cracks are produced. Larger energy ranges are preferable since they would necessitate less fine-tuning of the pecan cracking equipment.

4.2.1 Impactor geometry comparison

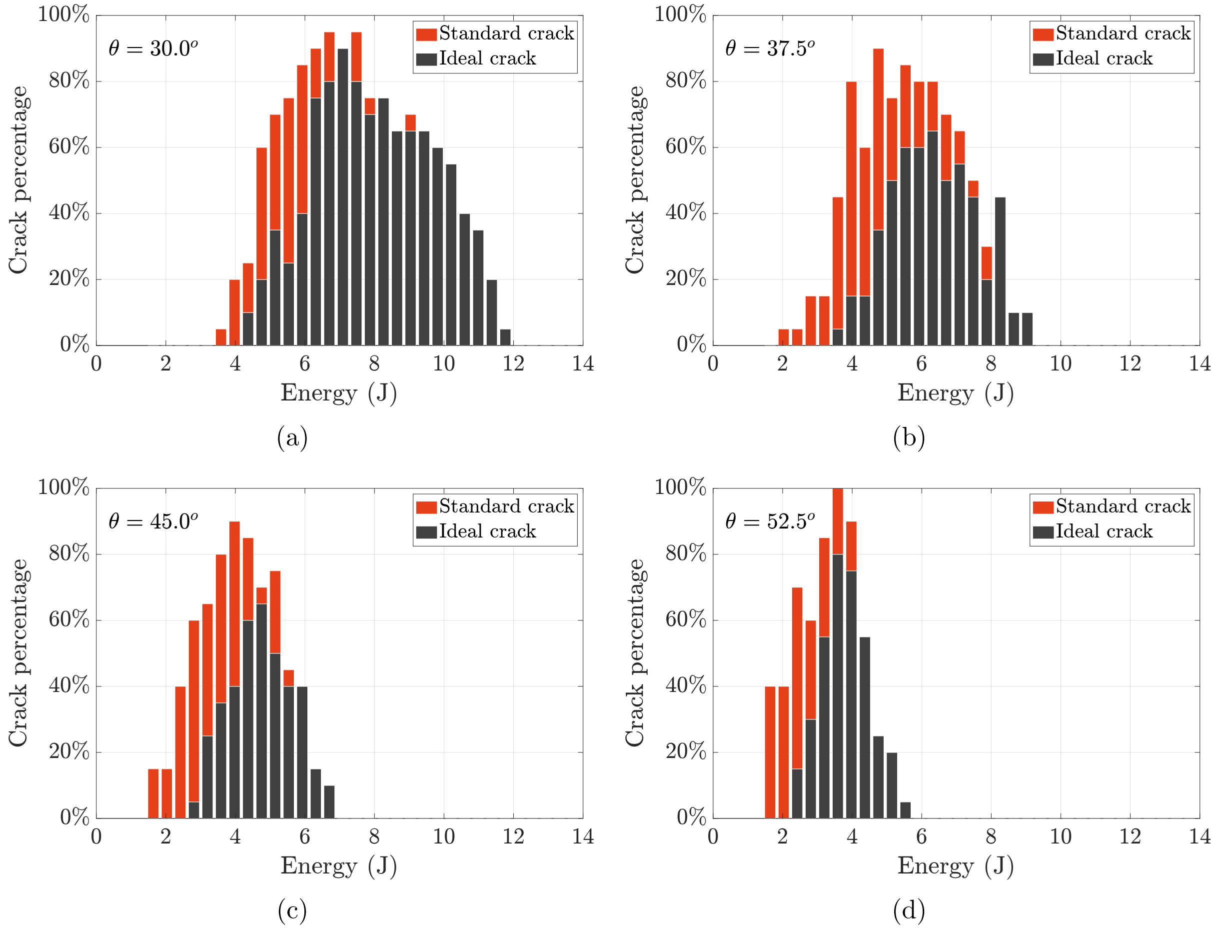

Figure 4.5. Percentage of standard and ideal cracks produced with each set of (a) 30.0° impactors, (b) 37.5° impactors, (c) 45.0° impactors, and (d) 52.5° impactors.

The percentage of standard and ideal cracks produced by each of the four impactors is shown versus the impactor energy in Figure 4.5. These results show that as the angle of the impactor increases, the optimal energy level for cracking decreases monotonically. Regarding the extent of the energy range over which a high percentage of standard and ideal cracks is produced, Figure 4.6 illustrates these ranges for each impactor geometry. The whiskers of the plot indicate the energy level beyond which zero standard or ideal cracks are produced. Below the left whisker, all pecans are classified as under cracked, and above the right whisker, all pecans are classified as over cracked. The width of each box indicates the energy range in which the majority (over 50%) of preferred cracks (standard and ideal) are produced. The vertical line inside each box indicates the energy level that produced the highest percentage of preferred cracks. The 30.0° impactor has the largest energy range of the four impactors. Similar to the trend observed in optimal energy level, the optimal energy range decreases as the impactor angle increases.

Figure 4.7 shows trends in optimal cracking energy and the energy range for optimal cracking (i.e., the box widths in Figure 4.6) with respect to the impactor internal angle. The similarity in these trends indicates that the energy range for optimal cracking is directly proportional to the optimal energy level. For example, if an impactor geometry requires a large amount of energy to sufficiently crack the nut, then there is a large range of target energy surrounding the optimal energy level. Further, it is observed that for small internal angles, changes to internal angle have cause larger changes to the target cracking energy and range, relative to impactors with larger internal angles.

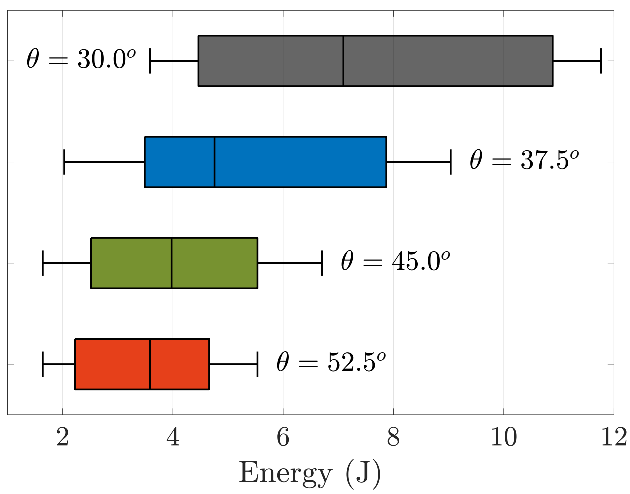

Figure 4.6. Energy ranges that produce more than 50% of the preferred (standard and ideal) crack types.

4.2.2 Impact energy analysis

To verify that impactor potential energy is an appropriate metric with which to study cracking trends, a sub-experiment is conducted in which impact energy is kept constant while varying the drop height and mass. Three drop masses are considered: 1.0 kg, 1.5 kg, and 2.0 kg. With energy constant, less massive drop weights will impact the pecan at a higher velocity since they are dropped from a greater height. The 45° impactor is used throughout the sub-experiment and the results are shown in Figure 4.8a-c. The results are presented as histograms showing the percentages of standard and ideal cracks obtained in each energy bin. The optimal energy range for each drop

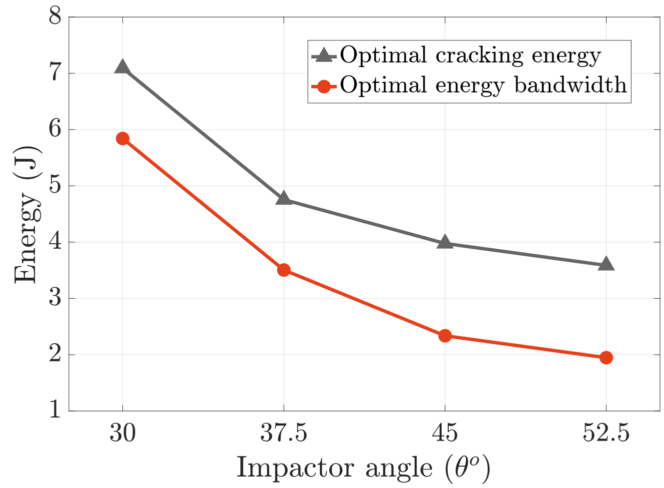

Figure 4.7. Optimal crack energy and 50% energy range versus impactor internal angle.

height and mass configuration are shown in Figure 4.8d. The relative similarity of the optimal energy ranges suggest that cracking trends are well captured by the single metric of impactor energy.

4.2.3 Crack length measurements

Figure 4.9 shows the average circumferential crack length in each energy bin for each impactor. The circumferential crack length is reported as the percentage of the circumference of the pecan. For standard and under cracked pecans, these ratios are calculated using the DCM software. For both ideal and over cracked pecans, the circumferential crack length is assigned a value of 100%. Uncracked pecans are assigned a circumferential crack length of 0%. Each curve ends at the energy level at which all the cracks produced are over cracked.

As the angle of the impactor decreases, the energy required to produce the same circumferential crack length increases. An average circumferential crack length of 50% occurs at 4.73 J for the 30.0° impactor, 3.90 J for the 37.5° impactor, 3.06 J for the 45.0° impactor, and 2.49 J for the 52.5° impactor. This trend in crack lengths is the same as that observed with crack distributions in Figure 4.5—for impactors with smaller internal angles, more energy is required to produce the same cracks. The curves in Figure 4.9 have similar energy ranges that produce circumferential crack lengths below 80%. However, impactors with smaller internal angles have a wider range of energy in which circumferential crack lengths between 80% and 100% are produced. It appears

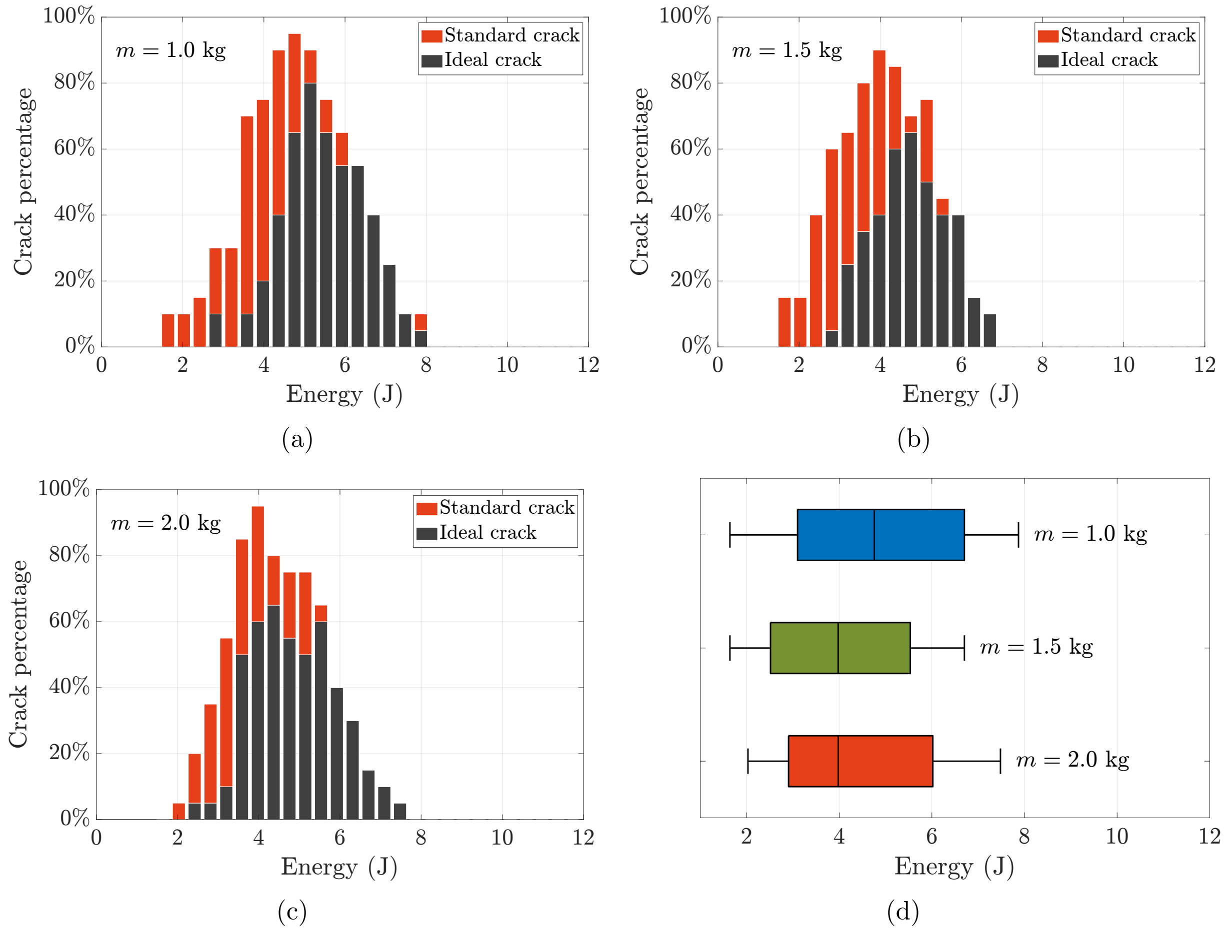

Figure 4.8. Percentage of standard and ideal cracks produced with a drop weight of mass (a) 1 kg, (b) 1.5 kg, or (c) 2 kg used to dropped on the impactors and (d) 50% energy ranges for each mass.

that impactors with smaller internal angles are less likely to over crack the pecan at higher energy ranges.

In general, impactors with smaller internal angles are less sensitive to changes in energy. It is hypothesized that these small-angle impactors would be advantageous in industrial cracking machines as they are more accommodating to variations in nut geometry, moisture level, and material properties.

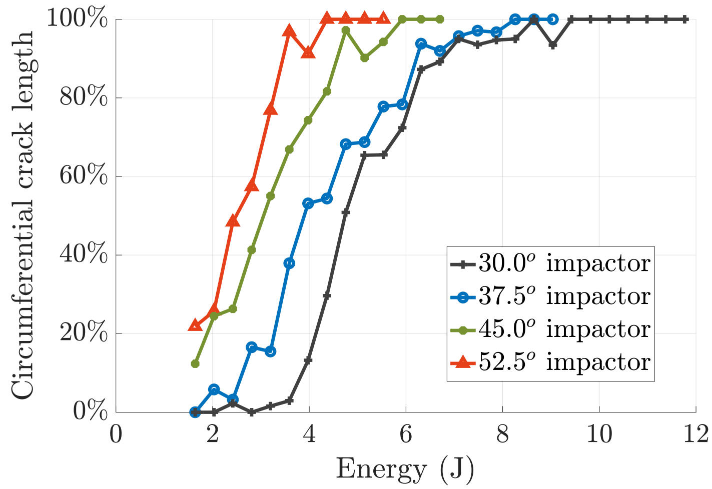

Figure 4.9. Percentage of pecan circumference cracked averaged at every energy level for each impactor geometry.

4.3 Overall impactor performance

Pecans are cracked with a set of four impactors with the following internal angles: 30.0°, 37.5°, 45.0°, and 52.5°. When comparing impactor geometries, it was found that 30.0° performed the best overall producing a total of 255 standard and ideal cracks. It outperformed the 37.5° impactor which produced 183 standard and ideal cracks, the 45.0° impactor which produced 141 standard and ideal cracks, and the 52.5° impactor which produced 118 standard and ideal cracks.

Chapter 5

Conclusion

5.1 Summary

The contributions of this thesis are organized into two key topics as follows:

1. Developing an image processing software for the detection, classification, and measurement of pecan cracks;

2. Determining optimal impact energy and impactor geometry for end-to-end pecan cracking for ease of shelling and reduction of kernel damage.

The DCM software provides an automated and consistent means to detect, classify, and measure pecan cracks. Crack detection is achieved by thresholding saturation values of each pixel in each frame and then applying noise reduction, stitching, and filtering of repeated cracks. Following crack detection, crack classification is achieved by observing crack orientation and area-to-length ratios. Once a crack is classified, different metrics were measured with the software for each crack type and were then measured experimentally for validation.

With the development of the DCM software, a multitude of tree nut cracking studies may be conducted with a reliable source of data that can be used to evaluate different methods. Before the introduction of this software, there was not a consistent way to measure a tree nut cracking process before the nuts are shelled. Moving forward, any research done on tree nuts can use this software to collect reliable data on cracks in the shells of nuts.

Additionally, nut cracking experiments were conducted to compare different pecan impactor geometries. The pecans were conditioned to a kernel moisture level of approximately 8%, placed between two end-to-end impactors, and cracked with an impulsive force delivered by a falling weight. The four internal angles of the pecan impactors considered were 30.0°, 37.5°, 45.0°, and 52.5°. The resulting crack types were categorized into four types: under crack, standard crack, ideal crack, and over crack, based on how easily the shell can be removed without damaging the kernel. The distribution of crack type and crack length is observed as a function of impact energy for each pecan impactor.

Based on its ability to produce a high percentage of preferred crack types across a relatively large energy range, the 30.0° impactor appears to be best suited for industrial end-to-end cracking. Currently, 45.0° impactors are the industry standard [45]. Since the 30.0° impactor can produce a high percentage of ideal cracks where the shell simply falls away from the kernel, it is recommended that processors implement a sorting stage to separate and secure intact and shelled kernels before sending the remaining nuts to a sheller.

5.2 Outlook

Pecans are one of the most difficult tree nuts to shell due to how fragile the kernels are and how tightly enclosed the kernels are in the shell. There is still a need to further tune cracking procedures so that a less aggressive shelling method can be used. There is also a need to research shelling procedures for pecans that are not as aggressive as the one described in this thesis. The results presented here suggest a better method of end-to-end pecan cracking that may be used to produce better cracks that can be shelled with current shelling methods.

Once a tuned cracking procedure is in place alongside a more sophisticated shelling procedure, it is possible that kernel yield becomes too great. Some customers, such as dessert manufacturers prefer to purchase pecans in pieces, so there is still a need to produce some pecan pieces to prevent needing to chop pecans to deliver on the need for pecan pieces. Ideally, a cracking or shelling method is to be devised that allows processors to tune the amount of kernel damage produced throughout the process.

Bibliography

[1] P. J. Conner and R. E. Worley, “Performance of 15 pecan cultivars and selections over 20 years in Southern Georgia,” *HortTechnology horttech*, vol. 12, no. 2, pp. 274 – 281, 2002.

[2] J. G. Woodroof, *Tree Nuts: Production, Processing, Products.* AVI Publishing Company, 1979.

[3] T. E. Thompson and P. J. Conner, “Pecan,” *Fruit breeding*, pp. 771–801, 2012.

[4] G. Ferrara, L. Lombardini, A. Mazzeo, and G. L. Bruno, “Evaluation of pecan [Carya illinoinensis (Wangenh.) K. Koch] cultivars for possible cultivation for both fruit and truffle production in the Puglia region, Southeastern Italy,” *Horticulturae*, vol. 9, no. 2, p. 261, 2023.

[5] A. G. Atanasov, S. M. Sabharanjak, G. Zengin, A. Mollica, A. Szostak, M. Simirgiotis, Łukasz Huminiecki, O. K. Horbanczuk, S. M. Nabavi, and A. Mocan, “Pecan nuts: A review of reported bioactivities and health effects,” *Trends in Food Science & Technology*, vol. 71, pp. 246–257, 2018.

[6] E. K. Heaton, A. L. Shewfelt, A. L. Badenhop, and L. R. Beuchat, “Pecan: handling, storage, processing and utilization,” *Research Bulletin-Georgia Experiment Station (USA)*, 1977.

[7] USDA, *Quick Stats*, United States Department of Agriculture: Sandersville, GA, USA, 2023.

[8] R. H. True, *Notes on the early history of the pecan in America.* US Government Printing Office, 1919.

[9] C. R. Santerre, *Pecan Technology.* Chapman & Hall, Inc., 1994.

[10] L. Wells, “Pecan planting trends in Georgia,” *HortTechnology*, vol. 24, no. 4, pp. 475–479, 2014.

[11] W. R. Forbus, S. D. Senter, and R. L. Wilson, "Physical properties of pecans relating to shelling efficency," *Journal of Food Science*, vol. 48, pp. 800–803, 1983.

[12] W. D. Goff, J. R. McVay, and W. S. Gazaway, *Pecan production in the southeast: a guide for growers.* University of Georgia Extension, 1989.

[13] O. Kabas and V. Vladut, "Determination of some engineering properties of pecan (*Carya illinoinensis*) for new design of cracking system," *Erwerbs-Obstbau*, vol. 58, pp. 31–39, 2015.

[14] C. Chengmao, S. Si, D. Ran, L. Bing, and W. Shuo, "Experimental study on mechanical characteristics of nut rupturing under impact loading," *International Journal of Agricultural and Biological Engineering*, vol. 10, pp. 53–60, 2017.

[15] X. Man, L. Li, Y. Zeng, Y. Tang, J. Yang, X. Fan, Y. Zhang, H. Zhang, G. Su, and J. Wang, "Mechanical impact characteristics of hollow shell granule based on continuous damage theory," *Powder Technology*, vol. 429, 2023.

[16] A. M. Olaniyan and K. Oje, "Some aspects of the mechanical proerties of shea nut," *Biosystems Engineering*, vol. 84, pp. 413–420, 2002.

[17] M. A. Koyuncu, K. Ekinci, and E. Sacran, "Cracking characterstics of walnut," *Biosystems Engineering*, vol. 87, pp. 305–311, 2004.

[18] S. E. Prussia, B. V. Verma, and W. M. Blum, "Shattering pecan shells with high-speed projectiles," *Transactions of the ASAE*, pp. 425–489, 1985.

[19] F. A. Oluwole, N. A. Aviara, and M. A. Haque, "Development and performance tests of a sheanut cracker," *Journal of Food Engineering*, vol. 65, pp. 117–123, 2004.

[20] B. S. Ogunsina, O. A. Koya, and O. O. Adeosun, "A table mounted device for cracking dika nut (*Irvingia gabonesis*)," *Agricultural Engineeering International: The CIGR Ejournal*, 2008.

[21] J. O. Olaoye and T. A. Adekanye, "Properties influencing cracking and separation of palm nuts in a mechanical cracker cum separator," *Croation Journal of Food Science and Technology*, vol. 10, 2018.

[22] W. Horwitz, *Official Methods of Analysis of the Association of Official Analytical Chemists*, vol. 13. Association of Official Analytical Chemists, 1980.

[23] E. Altuntas and Y. Özkan, “Physical and mechanical properties of some walnut (Juglans regia L.) cultivars,” *International Journal of Food Engineering*, vol. 4, no. 4, 2008.

[24] G. C. Braga, S. M. Couto, T. Hara, and J. T. P. A. Neto, “Mechanical behaviour of macadamia nut under compression loading,” *Journal of Agricultural Engineering Research*, vol. 72, pp. 239–245, 1999.

[25] W. R. Forbus and R. E. Smith, “Pecan conditioning methods for increased shelling efficiency,” *Transactions of the ASAE*, pp. 596–599, 1971.

[26] J. G. Woodroof and E. K. Heaton, *Pecans for Processing.* Georgia Agricultural Experiment Stations, 1961.

[27] H. K. Celik, N. Caglayan, and A. E. W. Rennie, “Nonlinear fem based high-speed shell shattering simulation for shelled edible agricultural products: Pecan fruit shattering,” *Journal of Food Process Engineering*, 2016.

[28] O. I. Okunola, O. J. Olukunle, O. A. A. Adetola, and W. Akinfiresoye, “The comparative analysis of a developed swing beater and conventional beater of a palm nut cracking machine,” *Turkish Journal of Agriculture - Food Science and Technology*, vol. 11, pp. 1298–1303, 2023.

[29] A. Mohan and S. Poobal, “Crack detection using image processing: A critical review and analysis,” *Alexandria Engineering Journal*, vol. 57, pp. 787–798, 2017.

[30] D. Ai, G. Jiang, S.-K. Lam, P. He, and C. Li, “Computer vision framework for crack detection of civil infrastructure—a review,” *Engineering Applications of Artificial Intelligence*, vol. 117, p. 105478, 2023.

[31] Y. Li, S. Dhakal, and Y. Peng, “A machine vision system for identification of micro-crack in egg shell,” *Journal of Food Engineering*, vol. 109, p. 127–134, 2012.

[32] K. Lawrence, S.-C. Yoon, G. Heitschmidt, D. Jones, and B. Park, "Imaging system with modified-pressure chamber for crack detection in shell eggs," *Sensing and Instrumentation for Food Quality and Safety*, vol. 2, pp. 116–122, 2008.

[33] J. Priyadumkol, C. Kittichaikarn, and S. Thainimit, "Crack detection on unwashed eggs using image processing," *Journal of Food Engineering*, vol. 209, pp. 76–82, 2017.

[34] R. Adhikari, O. Moselhi, and A. Bagchi, "Image-based retrieval of concrete crack properties for bridge inspection," *Automation in Construction*, vol. 39, pp. 180–194, 2014.

[35] X.-j. Xu and X.-n. Zhang, "Crack detection of reinforced concrete bridge using video image," *Journal of Central South University*, vol. 20, pp. 2605–2613, 2013.

[36] H.-N. Nguyen, T. Y. Kam, and P.-Y. Cheng, "An automatic approach for accurate edge detection of concrete crack utilizing 2d geometric features of crack," *Journal of Signal Processing Systems*, vol. 77, pp. 221–240, 2014.

[37] B. Shan, S. Zheng, and J. Ou, "A stereovision-based crack width detection approach for concrete surface assessment," *KSCE Journal of Civil Engineering*, vol. 20, pp. 803–812, 2015.

[38] R. G. Lins and S. N. Givigi, "Automatic crack detection and measurement based on image analysis," *IEEE Transactions on Instrumentation and Measurement*, vol. 65, no. 3, pp. 583–590, 2016.

[39] F. Ioli, A. Pinto, and L. Pinto, "UAV photogrammetry for metric evaluation of concrete bridge cracks," *ISPRS - International Archives of the Photogrammetry Remote Sensing and Spatial Information Sciences*, vol. XLIII-B2-2022, pp. 1025–1032, 2022.

[40] C. M. Langston, M. W. Jackson, and R. B. Davis, "An image processing method for the detection, classification and measurement of pecan cracks," *Under review in Measurement: Food*.

[41] W. Horwitz, *Official Methods of Analysis of the Association of Official Analytical Chemists*, vol. 13. Association of Official Analytical Chemists, 1980.

[42] P. F. Alcantarilla, A. Bartoli, and A. J. Davison, "Kaze features," in *Computer Vision–ECCV 2012: 12th European Conference on Computer Vision, Florence, Italy, Proceedings, Part VI 12*, pp. 214–227, Springer, 2012.

[43] M. W. Jackson, C. M. Langston, L. E. Madsen, and R. B. Davis, "The effect of impactor geometry on end-to-end pecan cracking," *AgriEngineering*, vol. 6, no. 3, pp. 2470–2480, 2024.

[44] P. J. Conner, "UGA variety test update: 'McMillan' shows promise for low-input plantings," *The Pecan Grower*, pp. 40–44, 2013.

[45] B. W. Savage, S. W. Savage, and R. D. Ingle, "Nut cracking apparatus," U.S. Patent 8,215,233 B2, Jul. 10, 2012.